Drug Development and Industrial Pharmacy, 35:408–416, 2009

ISSN: 0363-9045 print / 1520-5762 online
DOI: 10.1080/03639040802422096

informa
healthcare

Influence of Solid-State Acidity on the Decomposition of Sucrose in Amorphous Systems II (Effect of Buffer)

Khouloud A. Alkhamis

Department of Pharmaceutical Technology, Faculty of Pharmacy, Jordan University of Science and Technology, Irbid, Jordan

It was of interest to investigate the solid-state acidity using indicator probe molecules and sucrose degradation. Amorphous samples containing lactose, sucrose, buffers (citrate, malate, tartarate, or phosphate) with different pH values, and sodium chloride (to adjust the ionic strength) were prepared by freeze-drying. The lyophiles were characterized using powder X-ray diffraction, differential scanning calorimetry, and Karl Fischer titrimetry. The solid-state acidity of all lyophiles was measured using diffuse reflectance spectroscopy and suitable indicators (thymol blue or bromophenol blue). Selected lyophiles were subjected to a temperature of 60°C and were analyzed for sucrose degradation using the Trinder kit. The results obtained from this study have shown that good correlation can be obtained between the solid-state acidity and the molar ratio of the salt and the acid in solution. The degradation of sucrose in the lyophiles is extremely sensitive to the solid-state acidity and might be able to provide a better estimate for the acidity than the indicator probe molecules. The Hammett acidity-rate profile for sucrose degradation in the lyophiles (using four different buffers) was also obtained. The profile showed similarity to the pH-rate profile in solution, and no buffer catalysis for sucrose degradation was detected in this study.

Keywords solid state; acidity; buffer; cosolvent; polarity

INTRODUCTION

The chemical reactivity within the lyophiles is of great interest to pharmaceutical scientists, mainly because of its link to performance. In lyophilized formulations, there are several factors that are likely to influence the chemical reactivity. These factors include solid-state acidity, buffer catalysis, ionic strength, buffer crystallization, and molecular mobility. Therefore, the chemical reactivity (Badawy, 2001; Buera, Chirife, & Karel, 1995; Carstensen & Pothisiri, 1975; Chatterjee, 2004; Dublin, 1995; Flink, 1983; Glombitza & Schmidt, 1995; Karel & Labuza, 1968; Kouassi & Ross, 2000; Labuza, Schoebel, & Tannenbaum, 1969; Li, Guo, & Zografi, 2002; O'brien, 1996; Schebor, Buera, Chirife, & Karel, 1995; Townsend & Deluca, 1988), the solid-state acidity (Chatterjee, 2004; Glombitza, Oelkrug, & Schmidt, 1994; Li, Chatterjee, Medek, Shalaev, & Zografi, 2004; Scheef, Oelkrug, & Schmidt, 1998; Zinchuk et al., 2005), and buffer crystallization (Shalaev, Johnson-Elton, Chang, & Pikal, 2002) have been the subjects of many investigations.

Shalaev, Lu, Shalaeva, and Zografi (2000) studied the degradation behavior of sucrose in the solid state. The authors concluded that sucrose colyophilized with citric acid undergoes significant acid-catalyzed inversion at 50°C and that the rate of the reaction correlates with the initial solution pH. No attempts were made, in that study, to determine the acid–base characteristics of the citrate buffer after lyophilization.

In a previous study that was conducted by the same investigator of this study (Alkhamis, 2008) amorphous samples containing lactose, sucrose, citrate buffer, and sodium chloride were prepared by freeze-drying. The acidity in those lyophiles was determined and was correlated with the degradation rate of sucrose. The results obtained from the aforementioned study have shown that the solid-state acidity depends mainly on the molar ratio of sodium citrate and citric acid used in buffer preparation and not on the initial pH of the solution. The results also showed that the degradation of sucrose in the lyophiles is extremely sensitive to the solid-state acidity and the ionic strength.

The purpose of this study was to further investigate the relationship between the solid-state acidity and sucrose degradation using other buffers, namely, malate, tartarate, and phosphate. Each buffer was prepared at several pH values to cover the range of the particular buffer, and all experiments were conducted at a constant ionic strength.

MATERIALS AND METHODS

Materials

Sodium salts of thymol blue (TB) and bromophenol blue (BB), α-lactose monohydrate, sucrose >99.5%, anhydrous citric acid, phosphoric acid 85%, L-(–)-malic acid, L-(–)-malic

Address correspondence to Khouloud A. Alkhamis, Department of Pharmaceutical Technology, Faculty of Pharmacy, Jordan University of Science and Technology, Irbid 22110, Jordan. E-mail: khou@just.edu.jo

acids sodium salt, L-(+)-tartaric acid, sodium hydrogentartarate, and the anhydrous sodium dihydrogen citrate were all obtained from Sigma-Aldrich Co. (St. Louis, MO, USA). Sodium chloride, potassium phosphate monobasic and dibasic, and sodium citrate dihydrate tribasic were all obtained from Mallinckrodt Baker, Inc. (Phillipsburg, NJ or Paris, KY, USA). Glucose determination kit was obtained from Diagnostic chemicals Ltd. (Charlottetown, Prince Edward Island, Canada).

Methods

Lyophilization

Solutions containing lactose monohydrate (10%, wt/vol), sucrose (1%, wt/vol), 50 mM buffer (citrate, malate, tartarate, or phosphate), and sodium chloride (to adjust the ionic strength to 0.05 M), with an indicator (in case of acidity measurements) or without an indicator (in case of kinetic studies), were freeze-dried using a VirTis Advantage freeze-dryer (VirTis Co., Gardiner, NY, USA). The acids and the salts were used in different weight ratios in order to yield solutions with different pH values that cover the range of each particular buffer. The pH values of all solutions were measured using a pH meter (Oakton pH 500 Series, Fisher Scientific, USA) that was calibrated using standard buffers. In the freeze-dryer, the solutions were filled in 60-mL glass jars (~15 mL of solution per jar), cooled from room temperature to –40°C at 1°C/min, and held for 90 min. Primary drying was carried out at a shelf temperature of –40°C for 30 h and –30°C for 30 h, followed by an increase in the temperature to 0°C. Secondary drying was carried out at 45°C for 10 h. After lyophilization, the material was gently ground with a mortar and pestle in a glove box under nitrogen flow and was placed in a desiccator over anhydrous calcium sulfate (Drierite).

Spectra of the Indicators in Solution

The visible spectra for all samples were recorded using a Cary 100 Bio Spectrophotometer (Varian Inc., Mulgrave, Victoria, Australia) equipped with a diffuse reflectance accessory (model DRA-CA-301, Labsphere, North Sutton, NH, USA). Measurements were conducted over a wavelength range of 350–700 nm. The calibration curves were obtained by measuring the spectra of pH-adjusted indicator solutions (using phosphate or citrate buffers) containing either 0.0 or 25% (vol/vol) isopropyl alcohol (IPA). The concentration of the indicators used was 15 μg/mL. A buffer (with 0.0 or 25% [vol/vol] IPA and within the same pH range) was used for baseline correction (blank). The correlation between the solution pH and the log of the peak height ratio was then determined; the peak height ratio was defined as the basic peak maximum signal divided by the acidic peak maximum signal.

Spectra of the Indicators in Lyophiles

The diffuse reflectance spectra of the lyophiles were measured using a powder sample holder containing a quartz window. The approximate fill weight was 1.2 g, and the reflectance spectra of the lyophiles without the indicators were used for baseline correction. The relationships between the solution pH and the log of the peak height ratio were used to calculate the solid-state acidity of the lyophiles from their measured peak ratios.

Sucrose Inversion Kinetics

Assay Method. Glucose assay was performed by the Trinder method using a glucose determination kit. During analysis, 300 μL of each solution was taken and added to 5 mL of the reagent solution. The reagent solution was used as a blank, and the solutions were maintained at room temperature for 15 min to reach the colorimetric endpoint. Solutions were transferred to 1.4-mL quartz cuvette, and the absorbance was measured at 505 nm. Based on the measured glucose concentration, the unhydrolyzed sucrose concentrations in the lyophiles were calculated.

Kinetic Studies in Lyophiles. At the end of the freeze-drying cycle, the lyophiles were gently ground with a mortar and pestle in a glove box under nitrogen flow and were placed immediately in desiccators over anhydrous calcium sulfate (Drierite). The lyophiles were then maintained at 60°C in a temperature-controlled convective oven. Weighed amounts of the lyophiles (250–500 mg) were taken at time zero and at predetermined time intervals and were placed in 5 mL volumetric flasks, and 50 mM phosphate buffer (pH 6.5) was added to each flask to obtain a final volume of 5 mL. Samples were then analyzed using the Trinder kit and the method described above. No significant degradation during the analysis occurred due to the raise in the pH and the immediate analysis of the samples. No glucose was also detected at time zero.

X-Ray Powder Diffraction

All X-ray powder diffraction patterns of the lyophiles were collected by utilizing a Siemens X-ray diffractometer (Model D5005, Siemens). The radiation was generated by Cu Kα radiation filter at 45 kV and 40 mM. The samples were scanned from 5 to 45° 2θ, with a step size of 0.05 2θ and dwell time of 1 s. In all cases, initial and reacted samples exhibited no diffraction peaks and had the halo characteristic of a completely amorphous phase.

Water Content

At the end of the lyophilization, a weighed amount of each lyophile (~50 mg) was taken and a weighed amount of anhydrous methanol (~8 g) was added to it. The lyophile and the methanol were mixed very well, and then a known weight of the solution was injected into the titration vessel of a Karl Fischer Titrimeter. Based on the amount of the lyophile, the quantity of the added methanol, and the water content in the methanol blank, the water content of the lyophile was calculated. Water content (in the lyophiles) was also determined at the end of the kinetic study. At the end of the lyophilization, the average water content of the lyophiles was 1.4% ± 0.2, and it did not change substantially during the time course of the experiments.

Differential Scanning Calorimetry

A Differential Scanning Calorimetry with a refrigerated cooling accessory was used. The instrument was calibrated with indium. About 9–14 mg of the lyophiles were packed in aluminum pans and crimped. The samples were heated to 130°C at 10°C/min. The glass transition temperatures (T_g) were determined from the extrapolated onset of the endothermic step transition in the heating curve. All glass transition temperatures ranged from 73°C to 89°C and were at least 13°C higher than the temperature employed in the kinetic study.

RESULTS AND DISCUSSION

Acidity Measurements

The UV-visible spectra of TB and BB were collected over a range of solution pH values containing 0 and 25% (vol/vol) IPA. These spectra were used to construct pH versus peak ratio calibration curves. A typical plot is shown in Figure 1. The regression relationships obtained from the pH versus peak ratio plots, their effective pH range, and other relevant details are presented in Table 1. These relationships were used to calculate the Hammett acidity in the lyophiles.

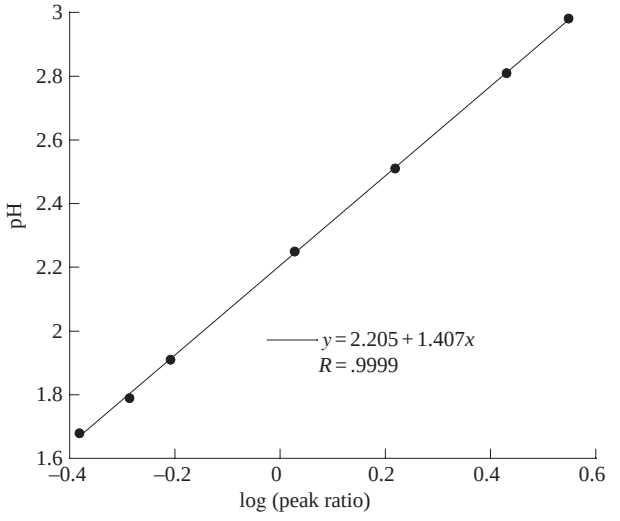

FIGURE 1. Solution pH versus log (peak ratio) plot for thymol blue in 25% isopropyl alcohol medium.

The pH values of the prelyo solutions, the composition of each buffer, and the Hammett acidity functions are shown in Tables 2–5. The composition of each buffer was obtained from the dissociation constants of the diprotic and the triprotic acids that were employed in this study. It is quite clear from Tables 2–5 that as the pH in the prelyo solutions is increased, the Hammett acidity (determined from either the cosolvent or the aqueous calibration plots) also increases. This result does not contradict what was previously obtained (Alkhamis, 2008) because the buffer concentration in this study is substantially high compared with the previous one. An attempt was also made to correlate the acidity in solutions (pH) and in lyophiles (Hammett function) with the molar ratio of salt to acid. In other words, an assumption is being made that the dibasic and the tribasic salts are negligible in the pH range that was employed in this study (less than 3% according to Tables 2–5). Excellent correlation was obtained between the pH in the prelyo solutions and the log (salt/acid) molar ratio used in buffer preparation (Figures 2–5). This result is expected according to the Henderson Hasselbalch equation. Good correlation was also observed between the Hammett acidity (obtained using the cosolvent calibration plots) and the log (salt/acid) molar ratio used in buffer preparation (Figures 2–4). However, the results obtained using phosphate buffer were less satisfactory (Figure 5), and it will be explained later in the kinetic study section. The results obtained from the aqueous calibration plots were also less satisfactory than those obtained using the cosolvent calibration plots. A typical plot is shown in Figure 6. This result also confirmed the previous conclusions regarding the cosolvent method and its ability to determine the solid-state acidity (Alkhamis, 2008). In Figures 2–5, the intercepts (for the prelyo solutions) were close to the pK_{a1} of each buffer. For example, for citrate buffer the intercept is 3.05, whereas the pK_{a1} value obtained from the literature is 3.128 (*The Merck index*, 1996). However, the slopes were less than the theoretical value of unity. This can be attributed to the low buffer concentration (0.05 M). In the lyophiles, the intercepts were lower than the pK_{a1} of each buffer in solution. This can be explained

TABLE 1
Indicator Properties and Calibration

Indicator	Medium	pH Range	Equation	R^2
Thymol blue	0.5 M phosphate buffer	1.53–2.53	[a]$y = 2.04 + 1.10x$	.999
Thymol blue	0.5 M phosphate buffer + 25% (vol/vol) IPA	1.68–2.98	[a]$y = 2.20 + 1.41x$	.999
Bromophenol blue	0.05 M citrate buffer	2.83–4.90	[a]$y = 3.56 + 0.904x$	.998
Bromophenol blue	0.05 M citrate buffer + 25% (vol/vol) IPA	3.21–5.26	[a]$y = 3.88 + 1.462x$	.991

[a]y = solution pH, $x = \log_{10}$ (signal ratio).

TABLE 2
Solution Composition of Citrate Buffer at Different pH Values (Estimated from the Dissociation Constants) and the Hammett Acidities of the Lyophiles

Measured pH in Prelyo Solutions	Citric acid (% Mole)	Monocitrate (% Mole)	Dicitrate (% Mole)	Tricitrate (% Mole)	Hammett Acidity[a]	Hammett Acidity[b]
2.46	82	18	—	—	1.74	1.68
2.55	79	21	—	—	1.92	1.82
2.66	75	25	—	—	2.11	1.97
2.79	69	31	—	—	2.28	2.11
2.95	60	40	—	—	2.51	2.71
3.11	51	48	1	—	2.87	2.93
3.29	40	58	2	—	3.13	3.09
3.46	31	66	3	—	3.42	3.27

$pK_{a1} = 3.128$, $pK_{a2} = 4.761$, $pK_{a3} = 6.396$.
[a]Cosolvent calibration plots.
[b]Aqueous calibration plots.

TABLE 3
Solution Composition of Malate Buffer at Different pH Values (Estimated from the Dissociation Constants) and the Hammett Acidities of the Lyophiles

Measured pH in Prelyo Solutions	Malic Acid (% Mole)	Monomalate (% Mole)	Dimalate (% Mole)	Hammett Acidity[a]	Hammett Acidity[b]
2.59	87	13	—	1.97	1.87
2.71	83	17	—	2.19	2.04
2.83	79	21	—	2.39	2.19
3.00	71	29	—	2.84	2.92
3.17	63	37	—	3.09	3.07
3.35	52	47	1	3.44	3.29
3.53	42	57	2	3.70	3.45
3.71	32	65	3	3.96	3.61

$pK_{a1} = 3.4$, $pK_{a2} = 5.1$.
[a]Cosolvent calibration plots.
[b]Aqueous calibration plots.

TABLE 4
Solution Composition of Tartarate Buffer at Different pH Values (Estimated from the Dissociation Constants) and the Hammett Acidities of the Lyophiles

Measured pH in Prelyo Solutions	Tartaric Acid (% Mole)	Monotartarate (% Mole)	Ditartarate (% Mole)	Hammett Acidity[a]	Hammett Acidity[b]
2.41	80	20	—	1.70	1.65
2.51	76	24	—	1.88	1.79
2.63	71	29	—	2.05	1.95
2.77	63	36	1	2.25	2.08
2.94	54	44	2	2.72	2.84
3.10	44	53	3	3.08	3.07

$pK_{a1} = 2.98$, $pK_{a2} = 4.34$.
[a]Cosolvent calibration plots.
[b]Aqueous calibration plots.

TABLE 5
Solution Composition of Phosphate Buffer at Different pH Values (Estimated from the Dissociation Constants) and the Hammett Acidities of the Lyophiles

Measured pH	Phosphoric Acid (% Mole)	Monophosphate (% Mole)	Diphosphate (% Mole)	Triphosphate (% Mole)	Hammett Acidity[a]	Hammett Acidity[b]
2.36	38	62	—	—	1.70	1.65
2.51	30	70	—	—	1.78	1.71
2.67	23	77	—	—	1.91	1.81
2.85	17	83	—	—	2.08	1.95
3.01	12	88	—	—	3.21	3.15
3.20	8	92	—	—	3.49	3.32
3.40	5	95	—	—	3.75	3.48
3.58	4	96	—	—	3.96	3.61
3.78	2	98	—	—	4.13	3.71

pK_{a1} = 2.15, pK_{a2} = 7.09, pK_{a3} = 12.32.
[a]Cosolvent calibration plots.
[b]Aqueous calibration plots.

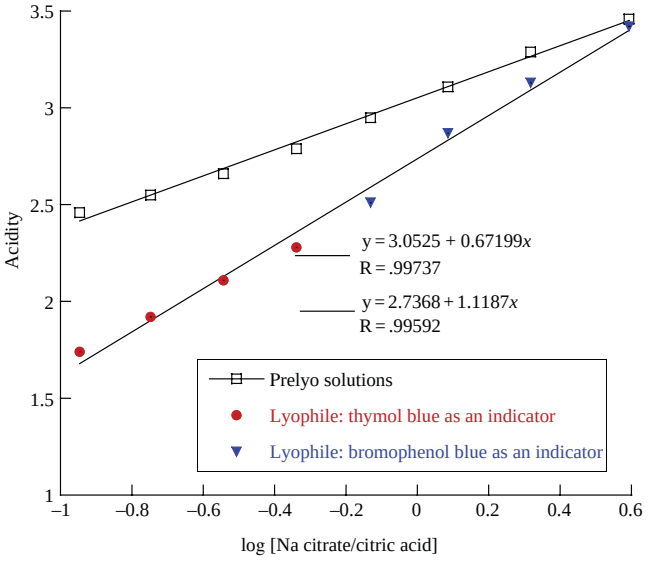

FIGURE 2. Acidity of the lyophiles and the prelyo solutions as a function of log [Na citrate/citric acid] molar ratio. The Hammett acidity was calculated using the cosolvent calibration plots.

as follows. In amorphous systems, the concepts of pH and pK_a are extended using the Hammett acidity function (Hammett, 1935):

$$H = \log\left[\frac{c_{A-}}{c_{HA}}\right]_L + pK_a = -\log a_H + \left[\frac{f_{A-}}{f_{HA}}\right] \quad (1)$$

where c, f, and a_H are the concentrations in the lyophiles, the activity coefficient, and proton activity, respectively. The molar ratio of the salt and acid in the lyophiles can be related to the molar ratio of the salt and acid in solution using the following equation:

$$\left[\frac{c_{A-}}{c_{HA}}\right]_L = \left[\frac{c_{A-}}{c_{HA}}\right]_S * \frac{1}{P} \quad (2)$$

where L is the lyophile, S is the prelyo solution, and P is a constant that reflects the shift in that ratio due to a shift in the polarity in the "near dry state" of the lyophile. Therefore, if the

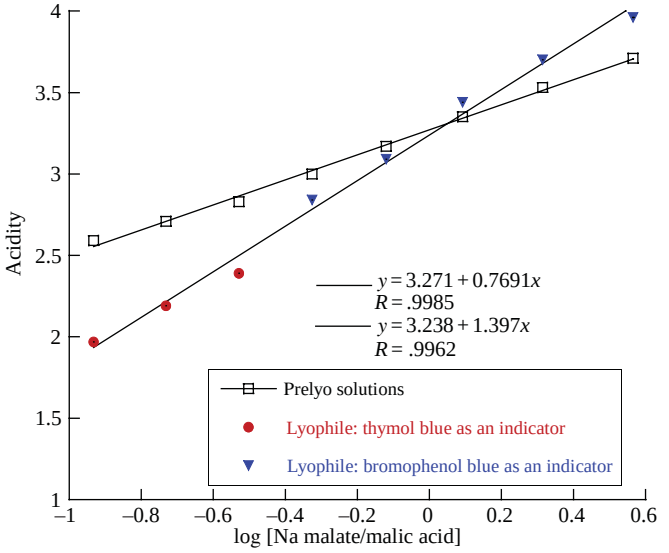

FIGURE 3. Acidity of the lyophiles and the prelyo solutions as a function of log [Na malate/malic acid] molar ratio. The Hammett acidity was calculated using the cosolvent calibration plots.

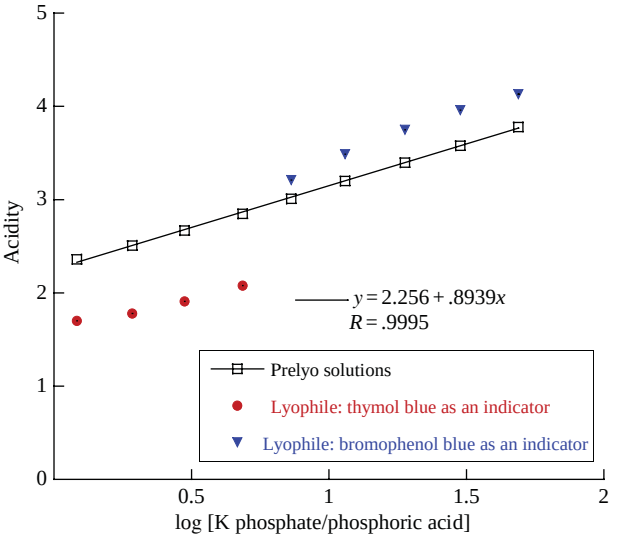

FIGURE 5. Acidity of the lyophiles and the prelyo solutions as a function of log [potassium phosphate/phosphoric acid] molar ratio. The Hammett acidity was calculated using the cosolvent calibration plots.

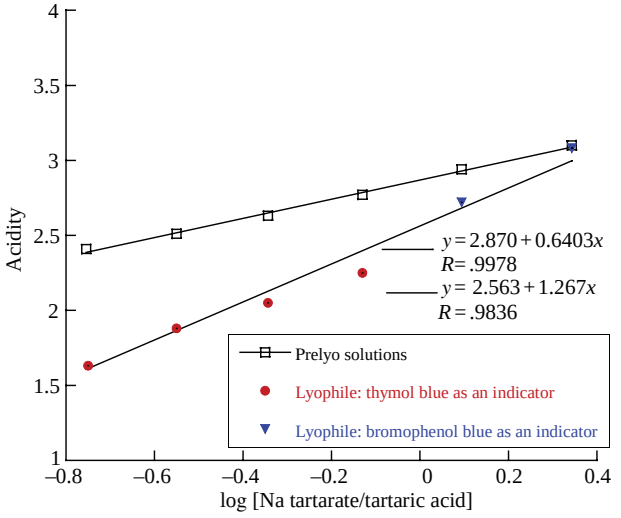

FIGURE 4. Acidity of the lyophiles and the prelyo solutions as a function of log [Na tartarate/tartaric acid] molar ratio. The Hammett acidity was calculated using the cosolvent calibration plots.

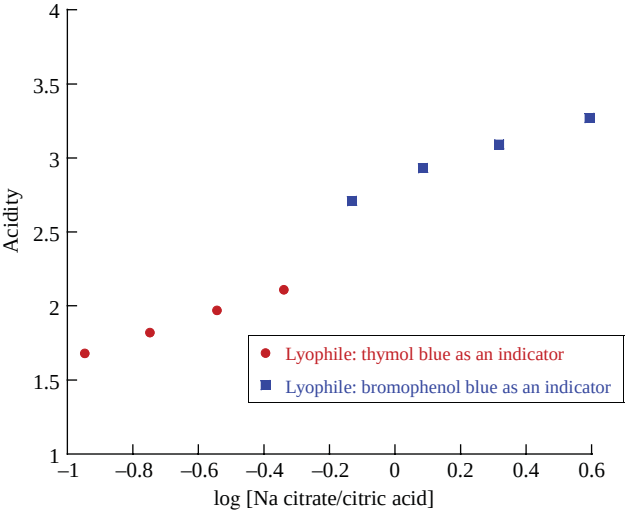

FIGURE 6. Acidity of the lyophiles as a function of log [Na citrate/citric acid] molar ratio. The Hammett acidity was calculated using the aqueous calibration plots.

polarity in the "near dry state" is less than the polarity in solution, then P is expected to be higher than 1. The Hammett acidity function can then be rewritten using the following equation:

$$H = \log\left(\left[\frac{c_{A-}}{c_{HA}}\right]_S * \frac{1}{P}\right) + pK_a \qquad (3)$$

The previous equation can be rearranged:

$$H = \log\left[\frac{c_{A-}}{c_{HA}}\right]_S + \log\frac{1}{P} + pK_a \qquad (4)$$

Therefore, a plot of the Hammett acidity versus log molar ratio of salt to acid in solution should give an intercept that reflects the pK_a and the shift in polarity in the lyophile. An intercept that is lower than the pK_{a1} of each buffer indicates that the polarity in

TABLE 6
The Reaction Rate Constants for Sucrose Degradation at Different pH Values and Hammett Acidities

Buffer	Indicator	Measured pH in Prelyo Solutions	Hammett Acidity	Reaction Rate Constant (h^{-1}) $\times 10^{-5}$	*R* Value
Citrate	Thymol blue	2.55	1.92	17.99	.9739
Malate	Thymol blue	2.59	1.97	15.50	.9822
Tartarate	Thymol blue	2.51	1.88	18.99	.9832
Phosphate	Thymol blue	2.51	1.78	21.48	.9840
Citrate	Bromophenol blue	3.11	2.87	5.31	.9821
Malate	Bromophenol blue	3.17	3.09	4.61	.9893
Tartarate	Bromophenol blue	3.10	3.08	5.52	.9887
Phosphate	Bromophenol blue	3.20	3.49	4.64	.9903

the lyophiles is less than the polarity in the prelyo solutions, and this result was observed in all buffers (citrate, malate, tartarate, and phosphate) that were employed in this study.

Sucrose Inversion Kinetics in the Lyophiles

The results obtained from the Hammett acidity versus the molar ratio for the phosphate buffer were less satisfactory than those obtained for citrate, malate, and tartarate buffers. It was obvious from Figure 5 that a straight line cannot be obtained over the entire Hammett acidity range. Also it was not clear, from the Hammett acidity measurements only, whether the shift in the acidity is real or whether one of the indicators or even both are not capable of determining accurately the Hammett acidity in the lyophiles that contain phosphate buffer. Therefore, it was decided to further investigate the behavior of the four buffers (citrate, malate, tartarate, and phosphate) in the lyophiles using sucrose degradation kinetics.

In a previous study that was conducted by the same investigator (Alkhamis, 2008), a conclusion was made that the degradation of sucrose in the lyophiles is extremely sensitive to the solid-state acidity. Therefore, eight lyophiles were selected for the kinetic study. The measured pH in the prelyo solutions and the Hammett acidity functions of these lyophiles are shown in Table 6. The measured solution pH values of the four buffers were within two narrow ranges (2.51–2.59 and 3.10–3.20). The kinetic curves for the loss of sucrose with time in these lyophiles are shown in Figures 7–8. First-order reaction rate constants of the lyophiles were determined from Figures 7–8 and the following equation:

$$C = C_0 \times e^{-kt} \tag{5}$$

where C, C_0, t, and k are the remaining concentration, the initial concentration, the time, and the reaction rate constant, respectively. The reaction rate constants for sucrose

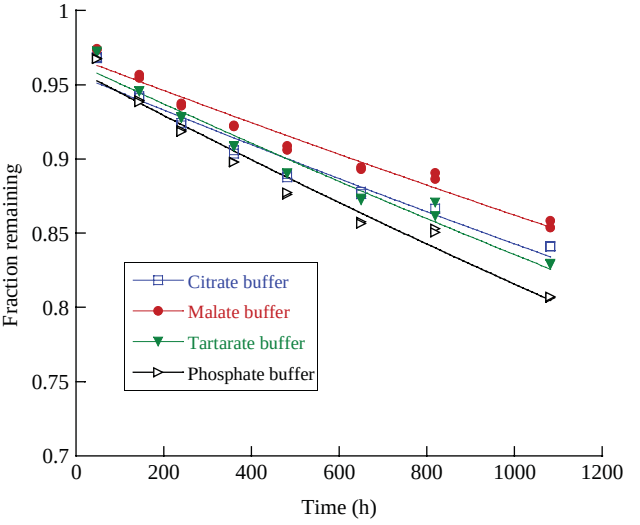

FIGURE 7. Sucrose hydrolysis in the freeze-dried samples. The Hammett acidities in these lyophiles were as follows: citrate buffer = 1.92, malate buffer = 1.97, tartarate buffer = 1.88, phosphate buffer = 1.78.

degradation in these lyophiles are also shown in Table 6. An attempt was made to correlate sucrose degradation with the Hammett acidity function in these lyophiles. This is shown in Figure 9. Excellent correlation was obtained between the reaction rate constants and the Hammett acidity functions using all buffers except the phosphate buffer at the higher acidity range (black square symbol). It is clear from Figure 9 that the Hammett acidity obtained using BB in the presence of phosphate buffer is overestimated. It is not conceivable at the moment what type of interaction between the BB and the phosphate buffer might be responsible for this erroneous result, and further studies might be needed to explain that interaction. However, in seven of eight cases (87.5%), the indicator probe molecules (TB and BB) were both successful in determining the solid-state acidity in the lyophiles.

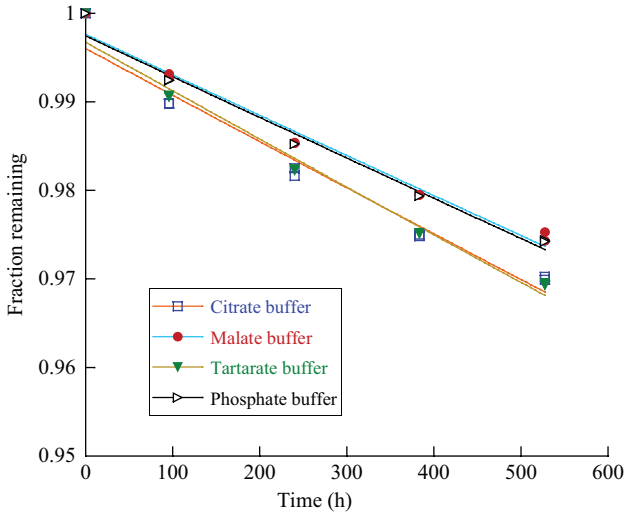

FIGURE 8. Sucrose hydrolysis in the freeze-dried samples. The Hammett acidities in these lyophiles were as follows: citrate buffer = 2.87, malate buffer = 3.09, tartarate buffer = 3.08, phosphate buffer = 3.49.

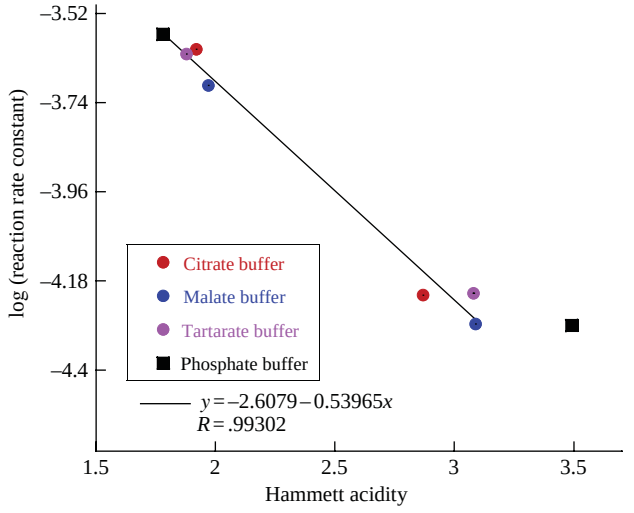

FIGURE 9. Hammett acidity-rate profile for the acid-catalyzed sucrose hydrolysis to glucose. The black square symbol (Hammett acidity = 3.49) was considered as an outlier and was not included in the linear regression.

CONCLUSIONS

This study has shown that the use of cosolvents (in the calibration plots) can provide a better estimate for the solid-state acidity than aqueous medium. It is further shown that good correlation can be obtained between the solid-state acidity and the molar ratio of the salt and the acid in solution. The solid-state acidities obtained using BB as an indicator probe molecule in the presence of phosphate buffer were overestimated. The degradation of sucrose in the lyophiles is extremely sensitive to the solid-state acidity and might be able to provide a better estimate for the acidity than the indicator probe molecules. The Hammett acidity-rate profile for sucrose degradation in the lyophiles (using four different buffers) was also obtained. The profile showed similarity to the pH-rate profile in solution, and no buffer catalysis for sucrose degradation was detected in this study.

ACKNOWLEDGMENT

The author thanks Professor Raj Suryanarayanan from the University of Minnesota and Dr. Evgenyi Shalaev from Pfizer Inc. for their help.

REFERENCES

Alkhamis, K. A. (2008). Influence of solid-state acidity on the decomposition of sucrose in amorphous systems (I). *Int. J. Pharm., 362*, 74–80.

Badawy, S. I. F. (2001). Effect of salt form on chemical stability of an ester prodrug of a glycoprotein IIb/IIIa receptor antagonist in solid dosage forms. *Int. J. Pharm., 223*, 81–87.

Buera, M. D. L., Chirife, J., & Karel, M. (1995). A study of acid-catalyzed sucrose hydrolysis in an amorphous polymeric matrix at reduced moisture contents. *Food Res. Intern., 28*(4), 359–365.

Carstensen, J. T., & Pothisiri, P. (1975). Decomposition of *p*-aminosalicylic acid in the solid state. *J. Pharm. Sci., 64*(1), 37–44.

Chatterjee, K. (2004). *Chemical reactivity and physical stability of lyophilized solids*. PhD thesis, University of Minnesota, MN.

Dublin, W. A. (1995). Degradation of bisoprolol fumarate in tablets formulated with dicalcium phosphate. *Drug Dev. Ind. Pharm., 21*(4), 393–409.

Flink, J. M. (1983). Nonenzymatic browning of freeze-dried sucrose. *J. Food Sci., 48*, 539–542.

Glombitza, B. W., & Schmidt, P. C. (1995). Surface acidity of solid pharmaceutical excipients II. Effect of the surface acidity on the decomposition rate of acetylsalicylic acid. *Eur. J. Pharm. Biopharm., 41*(2), 114–119.

Glombitza, B. W., Oelkrug, D., & Schmidt, P. C. (1994). Surface acidity of solid pharmaceutical excipients I. Determination of the surface acidity. *Eur. J. Pharm. Biopharm., 40*(5), 289–293.

Hammett, L. P. (1935). Reaction rates and indicator acidities. *Chem. Rev., 16*, 67–79.

Karel, M., & Labuza, T. P. (1968). Nonenzymatic browning in model systems containing sucrose. *J. Agric. Food Chem., 16*(5), 717–719.

Kouassi, K., & Ross, Y. H. (2000). Glass transition and water effects on sucrose inversion by invertase in a lactose-sucrose system. *J. Agric. Food Chem., 48*, 2461–2466.

Labuza, T. P., Schoebel, T., & Tannenbaum, S. R. (1969). Reaction at limited water concentration. 1. Sucrose hydrolysis. *J. Food Sci., 34*, 324–329.

Li, J., Chatterjee, K., Medek, A., Shalaev, E., & Zografi, G. (2004). Acid-base characteristics of bromophenol blue-citrate buffer systems in the amorphous state. *J. Pharm. Sci., 93*(3), 697–712.

Li, J., Guo, Y., & Zografi, G. (2002). Effects of a citrate buffer system on the solid-state chemical stability of lyophilized quinapril preparations. *Pharm. Res., 19*(1), 20–26.

O'brien, J. (1996). Stability of trehalose, sucrose and glucose to nonenzymatic browning in model systems. *J. Food Sci., 61*(4), 679–682.

Schebor, C., Buera, M. D. L., Chirife, J., & Karel, M. (1995). Sucrose hydrolysis in a glassy starch matrix. *Lebensm.-Wiss. U. Technol., 28*(2), 245–248.

Scheef, C. A., Oelkrug, D., & Schmidt, P. C. (1998). Surface acidity of solid pharmaceutical excipients III. Excipients for solid dosage forms. *Eur. J. Pharm. Biopharm., 46*, 209–213.

Shalaev, E. Y., Johnson-Elton, T. D., Chang, L., & Pikal, M. J. (2002). Thermophysical properties of pharmaceutically compatible buffers at sub-zero temperatures: Implications for freeze-drying. *Pharm. Res., 19*(2), 195–201.

Shalaev, E. Y., Lu, Q., Shalaeva, M., & Zografi, G. (2000). Acid-catalyzed inversion of sucrose in the amorphous state at very low levels of residual water. *Pharm. Res., 17*(3), 366–370.

The Merck index. (1996) (12th ed.). Whitehouse Station, NJ: Merck.

Townsend, M. W., & Deluca, P. P. (1988). Use of lyoprotectants in the freeze-drying of a model protein, ribonuclease A. *J. Parenter. Sci. Technol., 42*(6), 190–199.

Zinchuk, A. V., Hancock, B. C., Shalaev, E. Y., Reddy, R. D., Govindarajan, R., & Novak, E. (2005). The influence of measurement conditions on the Hammett acidity function of solid pharmaceutical excipients. *Eur. J. Pharm. Biopharm., 61*, 158–170.